ELSEVIER

Chemical Geology 177 (2001) 483–495

CHEMICAL GEOLOGY
INCLUDING
ISOTOPE GEOSCIENCE

www.elsevier.com/locate/chemgeo

Does δD from fluid inclusion in quartz reflect the original hydrothermal fluid?

Klaus Simon

Geochemisches Institut der Universität Göttingen, Goldschmidtstr. 1, 37077 Göttingen, Germany

Accepted 31 October 2000

Abstract

Hydrogen isotope investigations on hydrothermal quartz reveal two H-reservoirs: (i) trapped fluid inclusions, and (ii) structurally bound water in homogenously distributed small clusters or bubbles. Varying mixing ratios of the two reservoirs are sampled by means of mechanical and thermal decrepitation applied to different grain size fractions. A two-component mixing calculation results in an isotopic characterisation of the two H-reservoirs, which fractionate hydrogen isotopes close to the known MOH–H_2O system, with water being enriched in deuterium. Temperature controls both the internal fractionation as well as the abundance ratio of inclusion water to bonded water. At high temperatures, fractionation is small but bound water becomes more abundant, comprising a significant amount of water from both thermal and mechanical extraction techniques. Hence, the isotope composition of the extracted water does not reflect the original hydrogen isotope composition of the hydrothermal fluid especially at temperatures higher than 200°C. Previously reported δD data of fluid inclusion, which were used to elucidate the origin of the hydrothermal fluid, tend to be too low.

Keywords: Hydrogen; Deuterium; Stable isotopes; Fluid inclusions; Hydrothermal fluids; Quartz

1. Introduction

Hydrogen is one of the main trace constituents of quartz. From infra-red spectroscopic investigations by Brunner et al. (1961), Aines et al. (1984), Rovetta and Holloway (1986), and Cordier and Doukhan (1989) among others, it is well established that hydrogen is incorporated into quartz predominantly as (i) H_2O in fluid inclusions, and (ii) molecular H_2O or OH bonded to quartz surfaces. Aines et al. (1984) report that the molecular water is, in most cases, the major reservoir (< 3300 H/10^6 Si), exceeding OH^- by a factor of up to 20. Molecular water, which is thought to be randomly distributed throughout the crystal as bubbles of up to 0.2 μm, can be much more abundant than fluid inclusion water (McLaren et al., 1983). The overall water content can be close to zero in Brazilian quartz and as high as about 8% in low temperature microcrystalline agate (Flörke et al., 1982).

Hydrogen is the most suitable stable isotope system to monitor the origin and the conditions during hydrothermal precipitation. Numerous studies (Roedder, 1958; Kita, 1981; Kazahaya and Matsuo,

E-mail address: ksimon@gwdg.de (K. Simon).

0009-2541/01/$ - see front matter
PII: S0009-2541(00)00417-4

1985; Horita and Matsuo, 1986; Ohba and Matsuo, 1988) use different mechanical extraction techniques to measure the H isotope composition of the extracted waters. All these studies imply that the values represent the original isotopic composition of the hydrothermal fluids, although it is not evident from which sources within the quartz water or hydrogen is supplied. In addition, the fractionation processes occurring during formation as well as during cooling are yet not understood. To overcome differences in hydrogen isotope composition between fluid inclusion in quartz and associated minerals, different sources of fluids during precipitation have been attributed (Landis and Rye, 1974; Kamilli and Ohmoto, 1977; Bethke and Rye, 1979; Kelly and Rye, 1979). Foley et al. (1989) suggest a contamination of the primary inclusions population, with pseudosecondary inclusions trapped from shallow ground water. But as long as the incorporation and fractionation behaviour of hydrogen as H_2O, OH or H into quartz is not understood, these interpretation remain vague.

This study (i) reports a method to estimate the hydrogen isotopic composition of fluid inclusion water and structurally bonded water, (ii) discloses isotope fractionations in quartz, and (iii) shows that without knowledge of the internal distribution of H in quartz, the interpretation of δD in quartz data can be misleading.

2. Samples

Three quartz samples from the Mid-European Variscides have been investigated in detail, which were formed hydrothermally during different tectonic stages. The specific samples have been selected because sufficient amounts of homogenous sample material and microthermometric data (Hein, 1993, personal communication) are available, only one population of fluid inclusions have been incorporated during precipitation, and no secondary external overprint has occurred.

Milky white quartz 47/84 is from a hydrothermal main stage vein (qz3) of the "Grube Apollo, Stollen Alter Fritz", near Siegen (Germany) within the Rhenohercynian Zone of the Variscan Orogen. It is accompanied by siderite and sulfide ore deposits. Microthermometric measurements reveal only primary two phase aqueous low salinity fluid inclusions ($<$ 5% NaCl equiv.); the temperature of formation is estimated to be 300°C, though homogenisation temperatures are about 160°C (Hein, 1993). The sample Usingen is a zoned Kappenquartz with clear inclusion, poor and minor cloudy inclusion, rich parts made of two- and mono-phase secondary aqueous inclusions. It is from the post-tectonic Usingen quartz vein which transects the Taunus Mts. (Rhenish Massif) along 16 km. Microthermometric measurements reveal a highly saline fluid (20% NaCl equiv.). Temperature of formation is about 150°C similar to the homogenisation temperatures in the range from 110°C to 160°C (Behr and Horn, 1984). OW2c is a milky white to pink quartz sample from a vein within a syenite of the quarry Bitsch, Fürth-Erlenbach (Odenwald, Germany), which is placed in the Saxothuringian zone of the Variscan Orogen. Primary fluid inclusions (1–5 μm) are very rare, most are secondary (5–10 μm) two phase aqueous inclusions with a varying liquid–vapour ratio. Vapour-rich inclusions are characterized by homogenisation temperatures of about 110–160°C and salinities below 10%, water-rich inclusions have homogenisation temperatures within 180–220°C and salinities equal to 10–15% NaCl equiv. (Vratislav Huari, personal communication).

3. Methods

Quartz crystals have been crushed, selected for macroscopically homogenous portions, and sieved to various grain size fractions in the range between $>$ 0.09 and $<$ 3 mm. The fractions were hand-picked to remove visual impurities and further cleaned by common magnetic and gravity liquid separation techniques.

In order to gain refined information concerning the hydrogen isotopic composition and the water mass fractions of the different reservoirs, a method or a combination of methods to sample adequate volumes of a specific reservoir has to be developed. Smooth grinding of quartz is thought to preferentially liberate the water from fluid inclusions, especially large ones or those arranged in the plane of healed cracks. Decreasing grain size fractions of quartz correlate with a diminishing abundance of

large inclusions. Thermal decrepitation expels all H regardless of the position and type within the quartz structure. The application of thermal decrepitation to various grain size fractions yields waters with different mass contribution from fluid inclusion and structural water, and thus gives way to calculate the isotopic composition of the end members. Various methods for mechanical grinding process are described in the literature (Roedder, 1958; Kita, 1981; Kazahaya and Matsuo, 1985; Horita and Matsuo, 1986; Ohba and Matsuo, 1988). All of them report serious problems with adsorption of released water onto the newly formed quartz surfaces. Among other volatile gases, water is most effectively adsorbed (Barker and Torkelson, 1975). Adsorption is even more pronounced the larger the surface becomes during further grinding process. To improve the sampling technique, we designed a new grinding device operating like a pepper mill. There are several advantages relative to common ball mills: (i) the distribution of the grain sizes after grinding is confined to a very small range, which is controlled by manual adjustment of the clearance between rotor and stator, (ii) the time water is in physical contact with quartz is drastically reduced, and (iii) the duration of the extraction procedure is minimized to avoid full saturation of the newly formed surfaces, by adsorbing water expelled from inclusions, and to avoid further contamination by leaks to air moisture. Fig. 1 shows a simplified cross-section of the mill. The grinding stock is placed between a rotor and the encasement of stainless steel (stator). Quartz powder is sampled at the cylinder bottom. In addition, attached nozzle connects the cylinder with a cold trap. The top of the cylinder includes the axle drive shaft sealed with a gland of PTFE-bronze and Viton. Before and during the milling, the entire apparatus is heated up to a maximum of 190°C, to clean the initial quartz from adsorbed water and to minimize water adsorption during milling, respectively. Detailed adsorption experiments were performed to optimise grinding procedure and minimize adsorption processes. Fig. 2 shows the grain size spectrum after grinding for selected clearances. The results obtained for the isotopic composition and the water content show that the smaller the final grain sizes, the more enriched in deuterium the extracted water becomes; and the larger the final grain size, the smaller is the water yield.

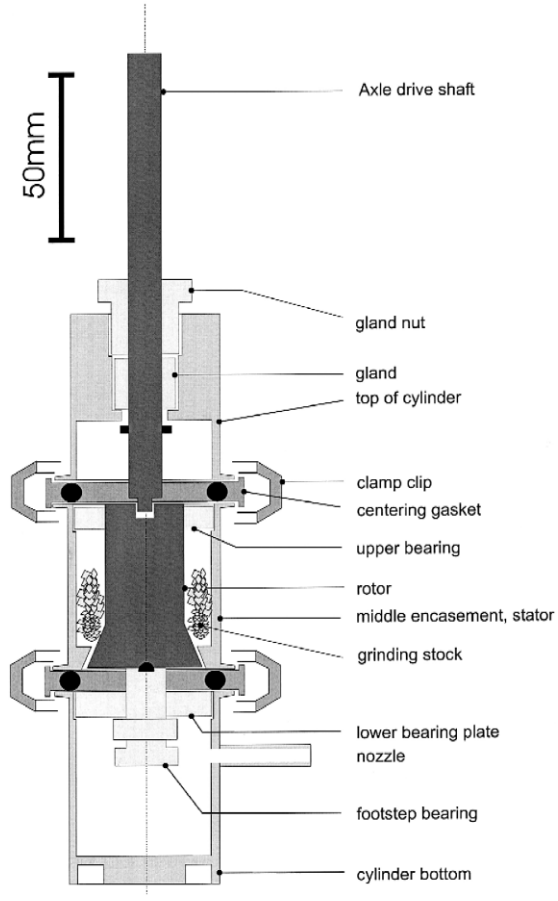

Fig. 1. Cross-section of the "pepper-mill" made of stainless steel.

For this reason, we only use a rather wide clearance of about 0.7–0.6 mm accepting a smaller water yield. At clearances of greater than 0.6 mm, the isotopic composition of the extracted waters does not vary very much and this value is similar to that achieved by thermal decrepitation as will be shown in more detail below. The adsorbed water is D-depleted and, therefore, the extracted water becomes more D-enriched the more adsorption occurs on the newly formed quartz surfaces during grinding.

3.1. Crushing

Aliquots of about 10 g of macroscopic homogenous sample material are dried for about 12 h at 190°C under vacuum conditions (10^{-3} mbar) in the milling apparatus to eliminate adsorbed air moisture

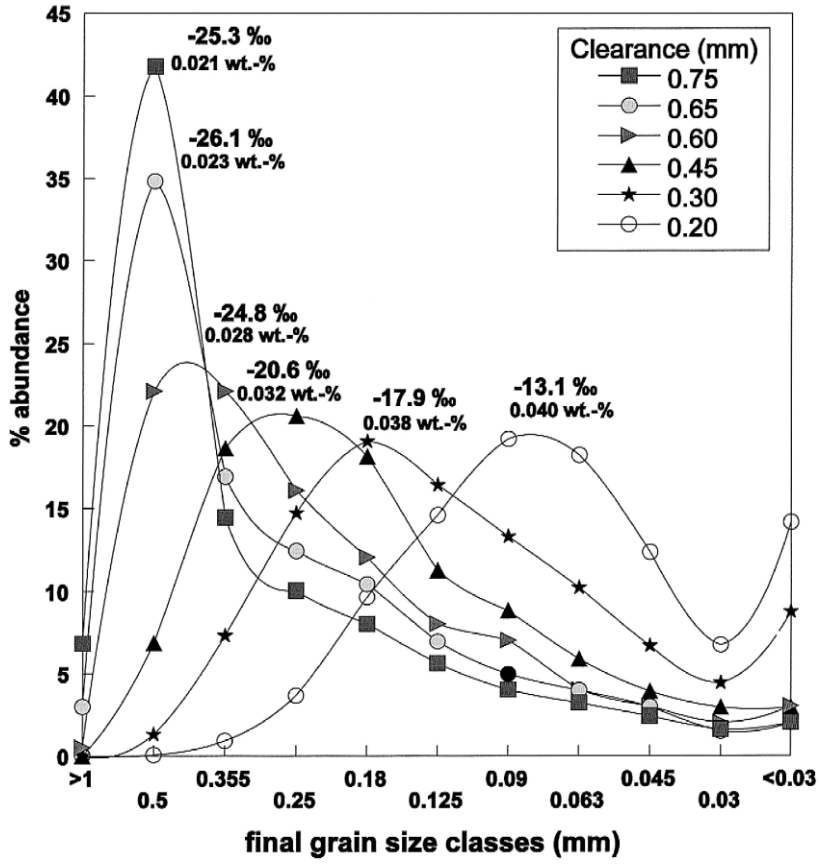

Fig. 2. Distribution of resulting grain size fractions after the grinding procedure, plotted against their frequency distribution in percent, illustrates the grinding and adsorption characteristics of the mill. The distribution of grain sizes after grinding is narrow, becoming smeared out at larger grinding degrees. Adsorption is evident by means of the hydrogen isotope δ-values of the extracted water which become enriched in D if newly formed surfaces become larger. Adsorption onto newly formed quartz surfaces enriches the extracted water in D, which is compatible with negative MOH–H_2O fractionation factors. Adsorption affects the δ-value only when the amount of newly formed surfaces is large relative to the amount of water extracted, i.e. when 50% of the resulting quartz powder is finer than 0.25 mm.

on the quartz surfaces. Then, the material was ground completely for about 1 min. The released water is trapped instantaneously at the cold finger attached to the nozzle. Further 10 min are required to complete the freezing of about 1–5 μl water onto the cold finger. This water is then transferred to a small volume Pyrex tube containing 150 mg Zn (Bloomington, Indiana University, USA). The glass tube containing water and zinc is closed and heated for 30 min to 500°C. Finally, the resulting H_2 gas is analysed immediately with a double inlet gas mass spectrometer Finnigan MAT 251. δD values are reported as per thousand (‰) deviation from V-SMOW. The error including water preparation and measurement is typically within $\pm$4‰.

3.2. Thermal decrepitation

Aliquots of about 5 g sample material are enclosed in a Molybdenum tube, dried for about 12 h at 150°C under vacuum conditions (10^{-3} mbar) to eliminate adsorbed air moisture, and then heated to 1200°C in an inductive oven. The extracted water is reduced to H_2 by hot uranium (850°C), adsorbed to activated charcoal at temperatures of liquid air, and immediately measured with the mass spectrometer.

4. Results and discussion

4.1. Water content

The extracted water content of the thermally extracted quartz fractions decreases monotonically as a function of the grain size (Table 1). The water contents of the samples range from a maximum value of 0.22 wt.% in 47/84 to a minimum value of 0.01 wt.% in Usingen quartz. Fig. 3 shows the water content in relation to the grain size fractions of the samples investigated. Sample 47/84 shows a steep gradient in water content as a function of decreasing grain sizes, whereas the slope of sample Usingen is very flat. Differences in slopes are related to the varying mixing ratio of fluid inclusion to molecular water. The differential change in water content becomes smaller with smaller grain size fractions. This suggests that the large fluid inclusions are eliminated during grinding and that the molecular bubbles become dominant in the small grain size fractions. Thus, thermal extraction of small grain size fractions predominantly supply molecular water. The water yield from the mechanical extraction procedure is much lower relative to the thermal extraction (grey symbols in Fig. 3). It can be seen that sample 47/84 shows much higher thermal yields in contrast to the mechanical procedure, whereas in sample Usingen, this difference is of minor importance. This observation corresponds with explanation of a large proportion of bubbles in sample 47/84 and of inclusion water in sample Usingen.

4.2. H isotope composition

From Fig. 4 and Table 1, it can be seen that the δD values of the thermally extracted waters decrease with decreasing grain size fraction. Values of samples 47/84 and OW2c asymptotically approach upper limits of −40‰ and −25‰, respectively, which show a close relationship to the δD values of the mechanically extracted waters (grey symbols in Fig. 4). The difference in isotopic composition between large and small grain sizes amounts to about 50‰ in Usingen and only 10‰ in 47/84.

From the combination of concentration (wt.% H_2O) and isotope data (δD), the molecular water content can be estimated, which is supposed to be constant for all grain sizes. A least-square mixing hyperbola as described in Albarède (1995) is calculated to fit the isotope and water data. The general equation of a hyperbola $(x_i - x_\infty)(y_i - y_\infty) = c$ with the asymptotes x_∞ and y_∞ and a constant c, characteristic of the curvature, states that the product of x

Table 1
Results obtained for the hydrogen isotope composition and water content of the various quartz grain size fractions for both thermal and mechanical extraction procedure

Size fraction (mm)	Method	Usingen		OW2c		47/84	
		δD (‰)	wt.% H_2O	δD (‰)	wt.% H_2O	δD (‰)	wt.% H_2O
0.063–0.09	thermal			−47	0.0502	−73	0.1387
0.09–0.125	thermal	−105	0.0099	−39	0.0559	−51	0.1217
0.125–0.18	thermal	−102	0.0093	−35	0.0621	−48	0.1348
0.18–0.25	thermal	−81	0.0116	−30	0.0637	−40	0.1364
0.25–0.35	thermal	−70	0.0137	−30	0.078	−43	0.1772
0.25–0.35	thermal	−89	0.007				
0.35–0.5	thermal	−68	0.0174	−25	0.0781	−42	0.1662
0.5–1.25	thermal			−25	0.086	−40	0.1803
1.25–2	thermal			−25	0.0915	−38	0.2138
2–3.5	thermal	−64	0.0262				
2–3.5	thermal	−60	0.028				
3.5–6.3	thermal	−52	0.042				
1.25–2	mechanical					−37	0.0536
2–3.5	mechanical			−18	0.0363		
3.5–6.3	mechanical	−49	0.016				

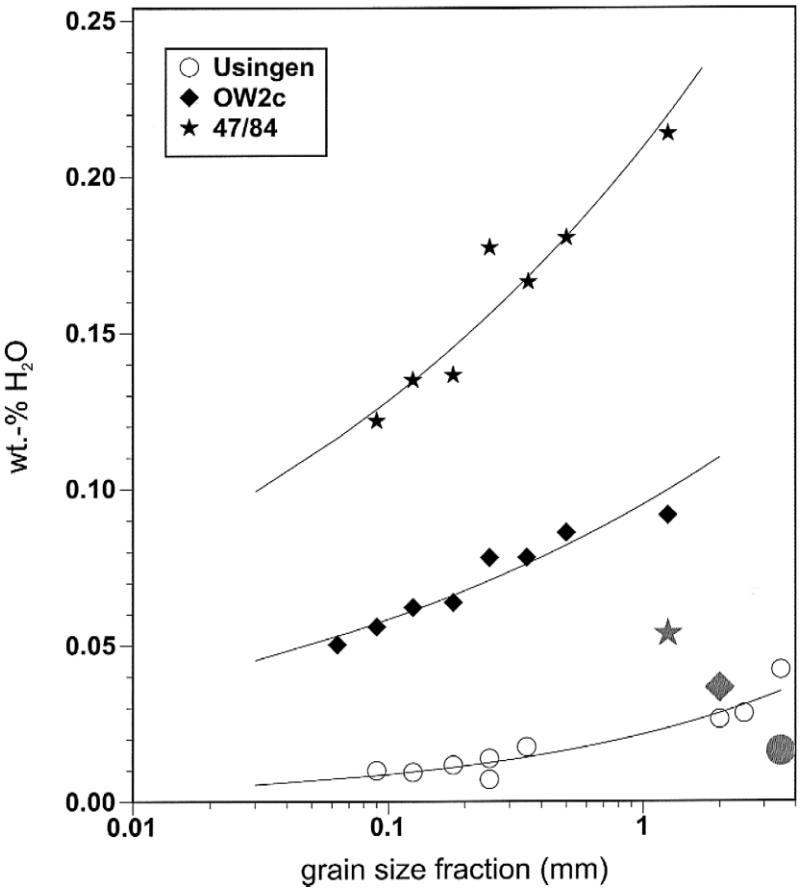

Fig. 3. H_2O content obtained by thermal decrepitation as a function of the log of the grain size fractions. The different slopes of the various samples indicate differences in the abundance ratio of fluid inclusion to molecular water. The grey symbols refer to the mechanically extracted water content which is always low compared to the thermal extraction.

and y is constant. Rewriting this equation for each pair of measurement yields $x_i y_i = c - x_\infty y_\infty + y_i x_\infty + x_i y_\infty$ corresponding to the matrix equation $\mathbf{y} = \mathbf{Ax}$ with

$$\mathbf{A} = \begin{vmatrix} 1 & y_1 & x_1 \\ 1 & \dots & \dots \\ 1 & y_n & x_n \end{vmatrix}, \quad \mathbf{x} = \begin{vmatrix} c - x_\infty y_\infty \\ x_\infty \\ y_\infty \end{vmatrix} \quad \text{and}$$

$$\mathbf{y} = \begin{vmatrix} x_1 y_1 \\ \dots \\ x_n y_n \end{vmatrix}.$$

The matrix is solved by $\mathbf{x} = (\mathbf{A}^T\mathbf{A})^{-1}\mathbf{A}^T\mathbf{y}$.

Fig. 5 exhibits the fitted data; the resulting parameters are summarized in Table 2.

The bubble water content defined by the x-asymptote varies in between a maximum value of 0.127 wt.% for sample 47/84 and a minimum value of 0.006 wt.% for sample Usingen. The y-asymptote corresponds to the hydrogen isotope composition of the total quartz and varies between −49‰ (Usingen), −39‰ (47/84), and −22‰ (OW2c).

The purpose of the following section is to estimate the hydrogen isotope composition of the end members, fluid inclusion, water and bubble water, respectively. With the molecular water content estimate in mind, a simple two reservoir mixing, which is mathematically described by a simple mass balance equation, is formulated.

$$\delta^i_{\text{total}} = \frac{C_{\text{bubble}}}{C^i_{\text{total}}}\delta_{\text{bubble}} + \frac{C^i_{\text{inclusion}}}{C^i_{\text{total}}}\delta_{\text{inclusion}}.$$

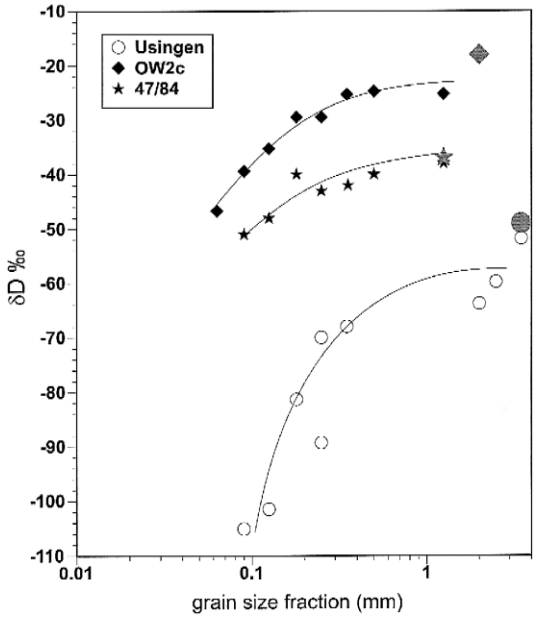

Fig. 4. δD values obtained by thermal decrepitation as a function of the log of the grain size fractions. The grey symbols refer to the isotopic composition of the mechanically extracted water.

δ-Values denote δD of extracted waters in per thousand (‰), C corresponds to the extracted water content as wt.%; subscripts denote total thermally extracted water (total), molecular water reservoir (bubble), inclusion fluid reservoir (inclusion), and superscript (i) variable parameters due to variable grain size fractions. For calculation, it is assumed that $C^i_{\text{total}} = C_{\text{bubble}} + C^i_{\text{inclusion}}$, because the distribution of bubbles due to their small size is independent of the grain size fraction. Thus, this equation can be transferred to:

$$\delta^i_{\text{total}} = \delta_{\text{bubble}} + \left(\frac{C^i_{\text{total}} - C_{\text{bubble}}}{C^i_{\text{total}}}\right) \times (\delta_{\text{inclusion}} - \delta_{\text{bubble}})$$

corresponding to a linear plot of δ^i_{total} on the Y-axes and $((C^i_{\text{total}} - C_{\text{bubble}})/C^i_{\text{total}})$ on the X-axes with slope $(\delta_{\text{inclusion}} - \delta_{\text{bubble}})$ and intercept δ_{bubble}.

Figs. 6–8 show the two-component mixing model for sample OW2c, Usingen, and 47/84, respectively. There is general agreement of data points with correlation coefficient of 0.953 (OW2c), 0.859 (Usingen), and 0.516 (47/84). Slope and intercept give an estimate of the hydrogen isotope composition of the fluid inclusion and bubble end member which are +3‰ and −48‰ for sample OW2c, −46‰ and −118‰ for sample Usingen, and −16‰ and −54‰ for sample 47/84. The calculated parameters are summarized in Table 2.

The inclusion to bubble mass ratio is inferred from the linear regression by inserting the δD value of the specific method or grain size in question. It

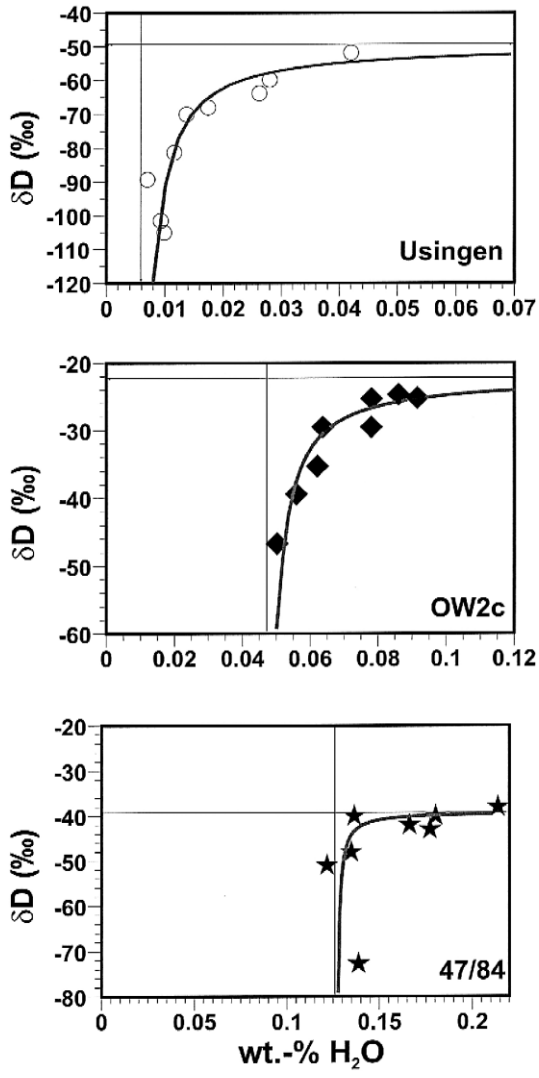

Fig. 5. Hyperbola mixing curve regression: the x- and y-asymptotes correspond to a lower limit of water content (structural water) and an upper limit in isotope composition (total system).

Table 2
Parameters obtained from (i) mixing hyperbola calculation, (ii) linear regression, (iii) microthermometry, (iv) extraction from large crystals, and (v) oxygen isotope measurements

	Usingen	OW2c	47/84
Mixing hyperbola			
C_{bubble} (x-asymptote) [wt.%]	0.0057	0.0465	0.1268
Curvature c	−0.18137	−0.14437	−0.04089
δD_{total} (y-asymptote) [‰]	−50	−22	−39
Linear regression of mass balance			
δD_{bubble} (intercept b) [‰]	−118	−48	−54
± Error δD_{bubble} [‰]	10	2	6
Δ ($\delta D_{inclsuion} - \delta D_{bubble}$) (slope m) [‰]	72	51	38
± Error Δ [‰]	16	7	26
$\delta D_{inclusion}$ ($m + b$) [‰]	−46	3	−16
± Error $\delta D_{inclusion}$ [‰]	26	9	31
Linear regression coefficient r^2	0.859	0.953	0.516
$C_{fluid\ inclusion}/C_{bubble}$ (thermal)	10	1	0.8
$C_{fluid\ inclusion}/C_{bubble}$ (mechanical)	10	1.6	0.8
Fluid inclusion microthermometry			
T of formation [°C]	150	200	300
Salinity [wt.% NaCl equiv.]	20	10	5
δD by extraction of large crystals			
δD thermal total [‰]	−52	−25	−38
δD mechanical total [‰]	−49	−18	−37
$\delta^{18}O$ values			
$\delta^{18}O$ quartz [‰ rel. V-SMOW]	17.6	11.3	18.4
$\delta^{18}O$ water [‰ rel. V-SMOW]	2.1	2.8	11.4

C_{bubble} is the wt.% content of the structural bond water; curvature c is a measure of the relative mass fractions of both reservoirs resulting from the calculation of the mixing hyperbola (see text for explanation), δD_{total} relates to the hydrogen isotope composition of the entire quartz. From the linear regression the intercept of the regression lines in Figs. 6–8 denotes the isotopic composition of the bubbles δD_{bubble} including error, the slope corresponding to the fractionation Δ between fluid inclusion water and structural water including error; $\delta D_{inclusion}$ is represented by the sum of slope and intercept with error; r^2 is the correlation coefficient of the linear regression; $C_{inclusion}/C_{bubble}$ refers to the mass ratio obtained by thermal decrepitation of the largest grain size fractions or mechanical decrepitation; temperature T of formation is derived from microthermometric measurements as well as the salinity of the fluid inclusions; $\delta D_{(thermal\ total)}$ is the measured isotope composition of the largest grain size fractions extracted thermally; $\delta D_{(mechanical)}$ is the mechanical extracted counterpart; $\delta^{18}O$ is the oxygen isotope composition of quartz and $\delta^{18}O$ is the value of water in equilibrium with quartz at temperature of formation.

varies between 10 and 0.8 for the mechanically extracted water and the thermal extraction water of the largest grain size fraction. Mechanical extraction still keeps a major reservoir of bubble water, but differs to a great extent relative to the total yield in the three samples investigated.

The content of bubble water defined through the regression line obviously depends on temperatures of formation (Table 2), which is in agreement with Griggs (1967), Paterson and Kekulawala (1979), Spear and Selverstone (1983), Paterson (1986) and Rovetta and Holloway (1986) who argued that temperature and pressure may control the solubilities of molecular water in quartz (increasing with increasing temperature and pressure). The lower the ratio of inclusion to bubble water, the higher are the temperatures of formation of fluid inclusion. The influence of salinity on the bubble content is not yet understood, but we suggest that incorporation of ions other than four-fold charged cause more defects to grow, which can be neutralised by more H^+ or OH^-.

4.3. Isotope fractionation

To our knowledge, hydrogen isotope fractionation factors for $Si(OH)_4$– or $Al(OH)_3$–water are not available in the literature. However, all known hy-

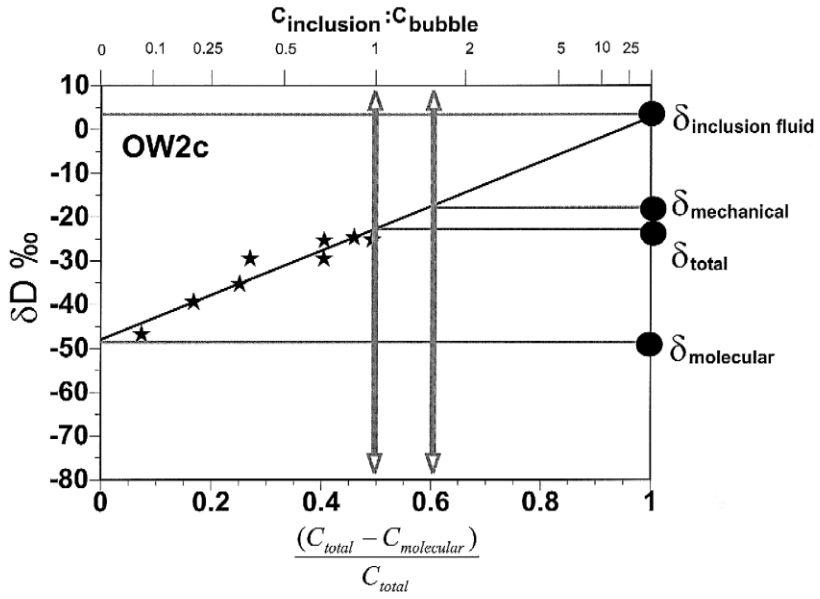

Fig. 6. Diagram of mass balance or two reservoir mixing for sample OW2c: intercepts for $x = 0$ and $x = 1$ are the extrapolated isotope compositions of structural and fluid inclusion water, respectively. δD measured with thermal and mechanical extraction method and calculated end member composition are denoted on the right hand side of the diagram. The relative mass ratios of both reservoirs are obtained by graphical solution of the regression with respect to $\delta D_{(mechanical)}$ and $\delta D_{(thermal\ total)}$. For further explanation, see text.

drogen isotope fractionation factors for OH-bearing Si- and Al-rich minerals, like muscovite and kaolinite and water, are negative and increase with decreasing temperature from about −10‰ at 400°C to −60‰ at 100°C (Suzuoki and Epstein, 1976; Liu and Epstein, 1984). Graham et al. (1980) point out

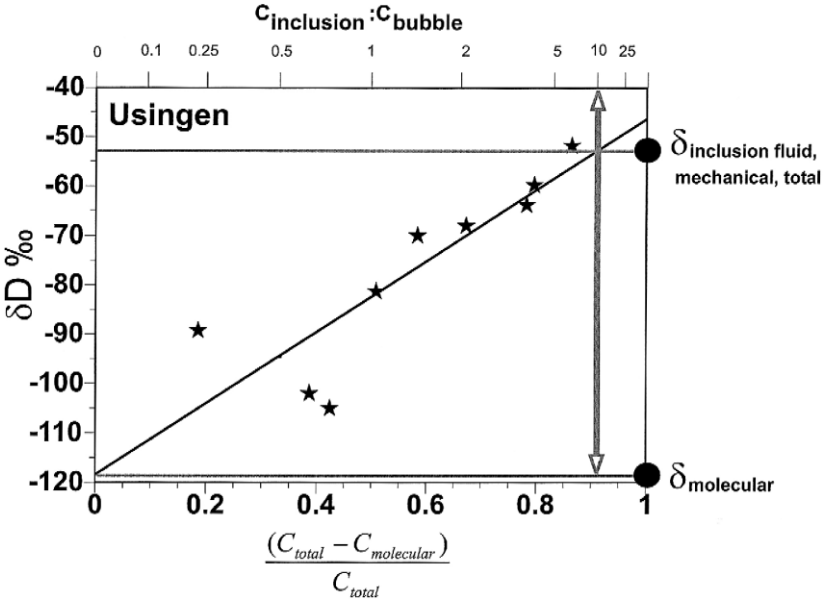

Fig. 7. Diagram of mass balance or two reservoir mixing for sample Usingen. Explanation as in Fig. 6.

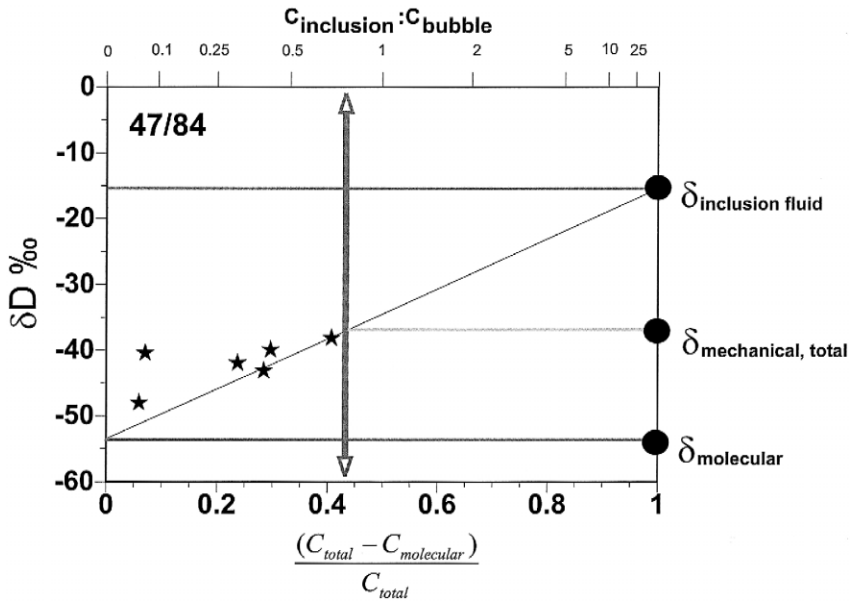

Fig. 8. Diagram of mass balance or two reservoir mixing for sample 47/84. Explanation as in Fig. 6.

that fractionation is not only a function of the octahedral site composition of the mineral, but also depends on the length and stereochemistry of hydrogen bonding in the mineral which have a marked influence on both the size of the mineral–water fractionation and the rate of isotopic exchange. Dobson et al. (1989) report fractionation factors between water vapour and dissolved water in silicate glasses that are even higher than for hydrous minerals and water.

As has been shown by the adsorption of isotopically light water on the newly formed quartz surfaces during the mechanical milling (Fig. 2), this fractionation behaviour holds true. This can be interpreted by means of adsorption of water partly as H_2O or OH to the quartz matrix. On the other hand, due to the very small surface to volume ratios in the bubbles, most of the water is in the form of H_2O or OH bound to the inner surface of this bubble, and even penetrating into the quartz matrix, building OH-halos leading to strong fractionation with respect to inclusion H_2O.

The estimated isotope fractionation between free trapped fluid inclusions water and structurally bound bubble water is between 72‰ and 38‰, and correlates with the temperatures of formation. This observation supports the idea that both reservoirs were formed during the precipitation of quartz and that the varying hydrogen isotope fractionation in the samples is the result of differences in temperatures of formation. A secondary build-up of fluid inclusion from the chemically bound water reservoir or vice versa is not plausible, because a fraction of about 50% of one reservoir is required to migrate through the lattice during cooling (as for sample 47/84). An independent trapping of two different generations of fluid inclusions at different times is also rejected for our samples.

Diffusion of hydrogen has been postulated to be an important process to modify the hydrogen isotope composition of quartz. Mavrogenes and Bodnar (1994) demonstrated hydrogen migration into and out of fluid inclusions during annealing and suggested that unexpectedly low δD values obtained from fluid inclusions were produced by the preferential movement of hydrogen relative to deuterium into fluid inclusions. Sterner et al. (1995) observed compositional changes of fluid inclusions without decrepitation during annealing at 3 kbar and 600–825°C, and demonstrated convincingly the chemical communication between fluids trapped as inclusions in quartz and an external fluid reservoir. Large channels that interconnect fluid inclusions have been observed by Bakker and Jansen (1990, 1991). A

mechanism for preferential leakage of fluid inclusions in quartz was presented by Bakker and Jansen (1994). Diffusion processes during cooling may stimulate re-equilibration, however, all authors agree that at temperatures below 400°C, the diffusion rate is slow; if the system is closed, the total hydrogen isotope composition is not changed, only the two reservoirs can be slightly shifted. For this reason, we accept that hydrothermal quartz has preserved the hydrogen isotope composition since formation.

Fig. 9 shows a summarizing cartoon of the inferred hydrogen isotope fractionation effects. The hydrothermal fluid precipitates quartz while fluid inclusions are mechanically trapped and molecular water is chemically bound. The isotope composition of the structural water depends on temperature and mass ratio of the two reservoirs, but is always depleted in D. As a consequence, the isotopic composition of the total water incorporated in quartz is lower than the original hydrothermal fluid. Internal re-equilibration during cooling can manipulate the isotopic composition of the reservoirs due to increasing fractionation. The measurements by thermal decrepitation of small grain size fractions yield far too low isotope ratios, the thermal decrepitation of large crystals result in the isotopic composition of the total system, but even the mechanical extracted water can be contaminated by bubble water and gives in most cases also erroneous δD values.

The hydrogen isotope composition of the sample Usingen with a low bubble water content yield comparable results for both mechanical and thermal total extracted water of about −50‰. Even the regressed value of the fluid inclusion end-member differs only within error. The bubble water content has only little influence on the isotopic composition of the bulk quartz although its isotopic composition is the lowest of all samples. The δ^{18}O value of quartz is 17.6‰, the δ^{18}O value of water in equilibrium at 150°C is about 2.1‰ (Zheng, 1993). These values characterize the hydrothermal water as a low temperature and high salinity metamorphic water of the Rhenoherzynian Zone.

Sample OW2c with increased bubble content shows larger discrepancies between the methods. The calculated δD values of end member fluid

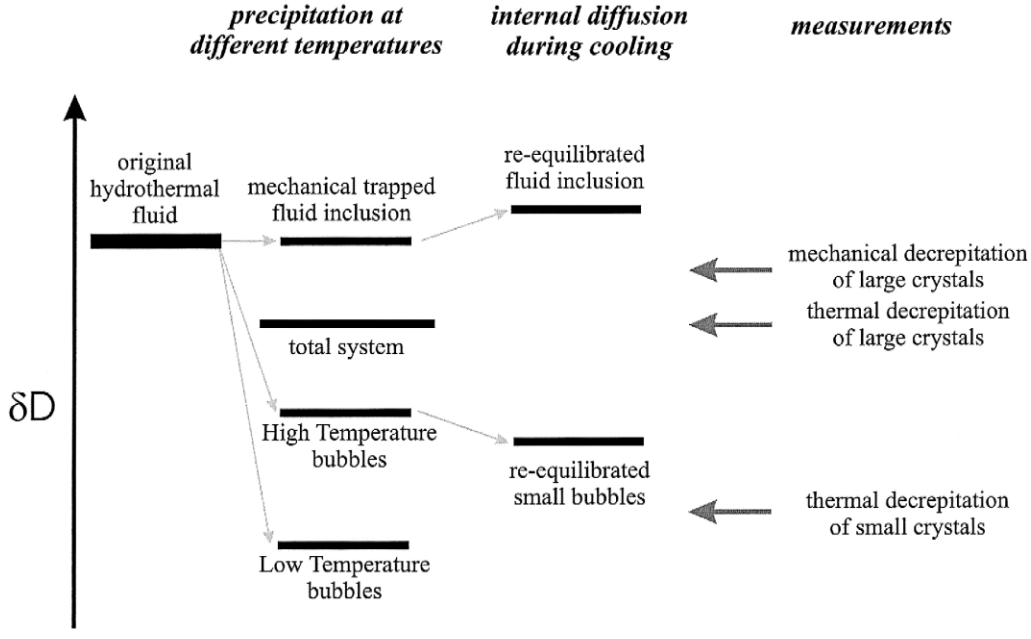

Fig. 9. Cartoon of the hydrogen isotope composition of fluid inclusion and structurally bound water due to fractionations during hydrothermal quartz precipitation and due to secondary internal diffusion and re-equilibration processes. Measurements by both extraction methods yield δD values different to the original hydrothermal fluid, but thermal and mechanical extraction on large grain sizes collects water not very much lower than the original hydrothermal fluid.

inclusion in OW2c is +3‰ (±9‰), whereas the mechanical extraction yields water with −18‰, thermal extraction of the largest grain sizes, −25‰, and even lower values for smaller grain sizes. From the $\delta^{18}O$ value of the quartz with 11.3‰, the water in equilibrium at 200°C is calculated to be about −0.3‰ (Zheng, 1993). This composition is similar to ocean water. This vein quartz within a syenite of the Saxothuringian Zone was presumably precipitated due to water rock interactions of the syenite with ocean water or precipitated from exsolved vapours from a salt-saturated brine of magmatic origin (Shmulovich et al., 1999).

Sample 47/84 has a calculated δD value of fluid inclusion of −16‰, but the mechanical and thermal extracted water show values of −37‰. The $\delta^{18}O$ value of quartz is 18.4‰; at temperatures of 300°C the hydrothermal water in equilibrium is 10.4‰ (Zheng, 1993). The isotopic composition of oxygen and hydrogen characterise this hydrothermal water as a high temperature and low salinity water of metamorphic origin.

In general, we suppose that the observed differences in hydrogen isotope composition between fluid inclusion in quartz and associated ore deposit minerals (Landis and Rye, 1974; Kamilli and Ohmoto, 1977; Bethke and Rye, 1979; Kelly and Rye, 1979) are due to the hydrogen isotope fractionation between H_2O and OH in quartz. Quartz is always reported to be the isotopically lightest mineral and the difference is always variable reaching up to about 30‰. To achieve more accurate δD estimates of the original hydrothermal fluid, one has to check the mass ratio of inclusion H_2O to the bubble H_2O/OH. If it is high and post entrapment diffusion of H is negligible, mechanical and thermal decrepitation of large grain sizes yield reasonable results; but if the ratio is low, one has to be aware that a significant contribution of isotopically light structural water causes erroneous δD values for the hydrothermal fluid.

5. Conclusion

During growth, hydrothermal quartzes incorporate mechanically trapped fluid inclusion water and structurally bound water. Because of hydrogen isotope fractionation between the hydrothermal fluid and the structurally bound water, the total hydrogen does not reflect the original hydrogen isotope composition of the precipitating hydrothermal fluid. A detailed study of the isotopic composition of varying mixing ratios of both reservoirs results in an evaluation of the isotopic composition of the end members, the fractionation factor between the reservoirs and their mass ratio in the crystal. Fractionation and mass ratio have been shown to correlate with temperature of formation and might serve as a pressure insensitive geothermometer. The calculated isotope composition of the extrapolated pure fluid inclusion water is the most probable δD value of the hydrothermal fluid. Thermal extraction of water in quartz even from large grain sizes with a high fluid inclusion to structural water ratio yields δD values which are up to 30‰ lower than the expected values. The largest deviations are found in high temperature quartzes because here the mass ratio of inclusion water to structurally bound water is low.

Acknowledgements

This research study was funded by the DFG grant Si 536/1. J. Hoefs is gratefully acknowledged for conclusive discussions and for the provision of lab facilities. The mechanical grinding device was developed by R. Skrandies and D. Curdt (Geochemisches Institut, Göttingen)). The author likes to thank U. Hein (IGDL, Göttingen) and V. Hurai (Geological Survey of Slovakia, Bratislava) who provided sample material and microthermometric data from OW2c. J. Horita and R.J. Bakker are thanked for thorough reviews and critical comments.

References

Aines, R.D., Kirby, S.H., Rossman, G.R., 1984. Hydrogen speciation in synthetic quartz. Phys. Chem. Miner. 11, 204–212.

Albarède, F., 1995. Introduction to Geochemical Modelling. Cambridge Univ. Press, Cambridge, UK, p. 262.

Bakker, R.J., Jansen, J.B.H., 1990. Preferential water leakage from fluid inclusions by means of mobile dislocations. Nature 345, 58–60.

Bakker, R.J., Jansen, J.B.H., 1991. Experimental post-entrapment

water loss from synthetic CO_2–H_2O inclusions in natural quartz. Geochim. Cosmochim. Acta 55, 2215–2230.

Bakker, R.J., Jansen, J.B.H., 1994. A mechanism for preferential H_2O leakage from fluid inclusions in quartz, based on TEM observations. Contrib. Mineral. Petrol. 116, 7–20.

Barker, C., Torkelson, B.E., 1975. Gas adsorption on crushed quartz and basalt. Geochim. Cosmochim. Acta 39, 212–218.

Behr, H.J., Horn, E.E., 1984. Unterscheidungskriterien für Mineralisationen des varistischen und postvaristischen Zyklus, die aus der Analyse fluider Einschlüsse gewinnbar sind. Postvaristische Gangmineralisationen in Mitteleuropa, Verlag Chemie, Weinheim, pp. 255–269.

Bethke, P.M., Rye, R.O., 1979. Environment of ore deposition in the Creede mining district, San Juan Mountains, Colorado: Part IV. Source of fluids from oxygen, hydrogen, and carbon isotope studies. Econ. Geol. 74, 1832–1851.

Brunner, G.O., Wondratschek, H., Laves, F., 1961. Ultrarotuntersuchungen über den Einbau von H in natürlichem Quarz. Z. Elektrochem. 65 (9), 735–750.

Cordier, P., Doukhan, J.C., 1989. Water solubility in quartz and its influence on ductility. Eur. J. Mineral. 1, 221–237.

Dobson, P., Epstein, S., Stolper, E.M., 1989. Hydrogen isotope fractionation between coexisting vapor and silicate glasses and melts at low pressure. Geochim. Cosmochim. Acta 53, 2723–2730.

Flörke, O.W., Köhler-Herberts, B., Langer, K., Tönges, I., 1982. Water in microcrystalline quartz of volcanic origin: agates. Contrib. Mineral. Petrol. 80, 324–333.

Foley, N.K., Bethke, P.M., Rye, R.O., 1989. A reinterpretation of the δD_{H2O} of inclusion fluids in contemporaneous quartz and sphalerite, Creede Mining District, Colorado: a generic problem for shallow ore bodies? Econ. Geol. 84, 166–177.

Graham, C.M., Sheppard, S.M.F., Heaton, T.H.E., 1980. Experimental hydrogen isotope studies I: systematics of hydrogen isotope fractionation in the systems epidote–H_2O, zoisite–H_2O and AlO(OH)–H_2O. Geochim. Cosmochim. Acta 44, 353–364.

Griggs, D.T., 1967. Hydrolytic weakening of quartz and other silicates. R. Astron. Soc. Am. Bull. 86, 846–852.

Hein, U.F., 1993. Synmetamorphic Variscan siderite mineralization of the Rhenish Massif, Central Europe. Min. Mag. 57, 451–467.

Horita, J., Matsuo, S., 1986. Extraction and isotopic analysis of fluid inclusions in halites. Geochem. J. 20, 261–272.

Kamilli, R.J., Ohmoto, H., 1977. Paragenesis, fluid inclusion, and isotope studies of the Finlandia vein, Colqui district, central Peru. Econ. Geol. 72, 950–982.

Kazahaya, K., Matsuo, S., 1985. A new ball-milling method for the extraction of fluid inclusions from minerals. Geochem. J. 19, 45–54.

Kelly, W.C., Rye, R.O., 1979. Geologic, fluid inclusion, and stable isotope studies of the tin–tungsten deposits of Panasqueira, Portugal. Econ. Geol. 74, 1721–1822.

Kita, I., 1981. A new type ball mill made of pyrex glass. Geochem. J. 15, 289–291.

Landis, G.P., Rye, R.O., 1974. Geologic, fluid inclusion, and stable isotope studies of the Pasto Bueno tungsten-base metal ore deposit, northern Peru. Econ. Geol. 69, 1025–1059.

Liu, K.K., Epstein, S., 1984. The hydrogen isotope fractionation between kaolinite and water. Isot. Geosci. 2, 335–350.

Mavrogenes, J.A., Bodnar, R.J., 1994. Hydrogen movement into and out of fluid inclusions in quartz: experimental evidence and geologic implications. Geochim. Cosmochim. Acta 58, 141–148.

McLaren, A.C., Cook, R.F., Hyde, S.T., Tobin, R.C., 1983. The mechanism of the formation and growth of water bubbles and associated loops in synthetic quartz. Phys. Chem. Miner. 9, 79–94.

Ohba, T., Matsuo, S., 1988. Precise determination of hydrogen and oxygen isotope ratios of water in fluid inclusions of quartz and halite. Geochem. J. 22, 55–68.

Paterson, M.S., 1986. The thermodynamics of water in quartz. Phys. Chem. Miner. 13, 245–255.

Paterson, M.S., Kekulawala, K.R.S.S., 1979. The role of water in quartz deformation. Bull. Mineral. 102, 92–98.

Roedder, E., 1958. Technique for the extraction and partial chemical analysis of fluid-filled inclusions from minerals. Econ. Geol. 53, 235–269.

Rovetta, M.R., Holloway, J.R., 1986. Solubility of hydroxyl in natural quartz annealed in water at 900°C and 1.5 GPa. Geophys. Res. Lett. 13 (1), 145–148.

Shmulovich, K.I., Landwehr, D., Simon, K., Heinrich, W., 1999. Stable isotope fractionation between liquid and vapour in water–salt systems up to 600°C. Chem. Geol. 157, 343–354.

Spear, F.S., Selverstone, J., 1983. Water exsolution from quartz: implications for the generation of retrograde metamorphic fluids. Geology 11, 82–85.

Sterner, S.M., Hall, D.L., Keppler, H., 1995. Compositional reequilibration of fluid inclusions in quartz. Contrib. Mineral. Petrol. 119, 1–15.

Suzuoki, T., Epstein, S., 1976. Hydrogen isotope fractionation between OH-bearing minerals and water. Geochim. Cosmochim. Acta 40, 1229–1240.

Zheng, Y.F., 1993. Calculation of oxygen isotope fractionation in anhydrous silicate minerals. Geochim. Cosmochim. Acta 57, 1079–1091.